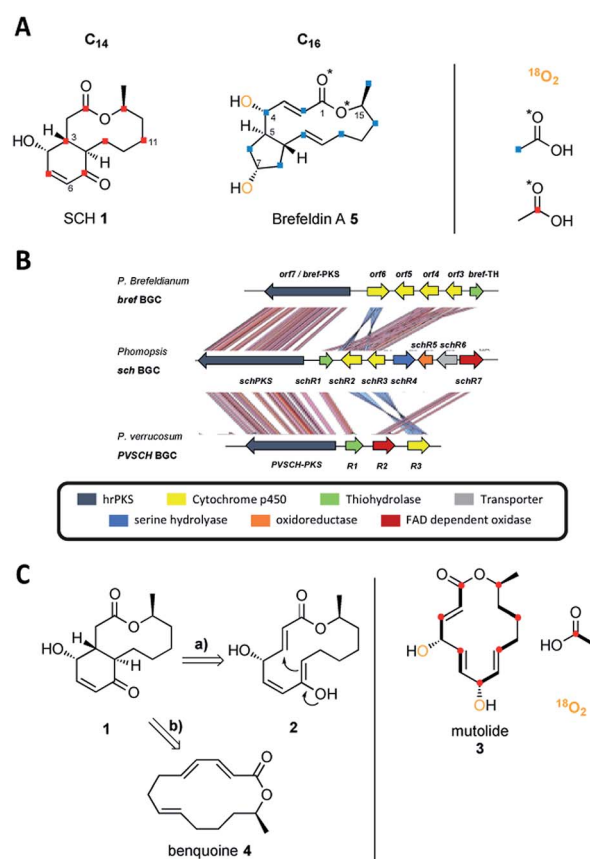Check for updates

Investigating the biosynthesis of Sch-642305 in the fungus *Phomopsis* sp. CMU-LMA†

Francesco Trenti,‡[a] Karen E. Lebe,[a] Emilie Adelin,[b] Jamal Ouazzani,[b] Carsten Schotte*[a] and Russell J. Cox [ID] *[a]

Sch-642305 is an unusual bicyclic 10-membered macrolide produced by the filamentous fungus *Phomopsis* sp. CMU-LMA for which no biosynthetic evidence exists. Here, we generate a draft genome sequence of the producing organism and discover the biosynthetic gene cluster responsible for formation of Sch-642305. Targeted gene disruptions together with reconstitution of the pathway in the heterologous host *Aspergillus oryzae* dissect key chemical steps and shed light on a series of oxidoreductions occuring in the pathway.

Introduction

Fungal polyketides are one of the most important classes of secondary metabolites, displaying both high structural diversity and a broad range of biological activities.[1] Among these Sch-642305 (SCH **1**, Scheme 1A) is an unusual bicyclic 10-membered macrolide produced by various filamentous fungi.[2–4] It displays potent inhibitory activity against both bacterial DNA primase ($EC_{50} = 70$ μM) and HIV-1 Tat ($IC_{50} = 1$ μM), making it an attractive target in the ongoing search for novel treatments of bacterial and viral infections.[2,4] Since its initial discovery from the filamentous fungus *Penicillium verrucosum* in 2003 (ref. 2) it has attracted the interest of synthetic chemists and several synthetic approaches towards SCH **1** have been reported.[5–7] A 'biomimetic' synthesis of SCH **1** was reported by Snider and Zhou based on a key transannular Michael cyclization of the 14-membered lactone **2** to generate the bicyclic scaffold of SCH **1** (Scheme 1C and ESI Fig. S1†), although it is not known if the biosynthesis does, in fact, involve a transannular Michael reaction.[8] Lactone **2** is structurally related to the fungal metabolite mutolide **3**, a highly reduced polyketide 2,5,8-triene lactone possessing the same number of carbons as SCH **1** (Scheme 1C). Mutolide **3** was shown by labelling experiments to be derived from seven acetate/malonate units and both hydroxyl groups are derived from atmospheric oxygen, suggesting post-

[a]Institute for Organic Chemistry and BMWZ, Leibniz Universität Hannover, Schneiderberg 38, 30167, Hannover, Germany. E-mail: russell.cox@oci. uni-hannover.de

[b]Centre National de la Recherche Scientifique, Institut de Chimie des Substances Naturelles ICSN, Gif-sur-Yvette, France

† Electronic supplementary information (ESI) available. See DOI: 10.1039/d0ra05311b

‡ Current address: Max Planck Institute for Chemical Ecology, Department of Natural Product Biosynthesis, Jena.

Scheme 1 A) Incorporation of labelled acetates and $^{18}O_2$ into SCH **1** and brefeldin A **5**; (B) *sch* biosynthetic gene cluster and comparison to the *bref* BGC and *PVSCH* BGC; (C) hypothetical biosynthetic route to SCH **1** proposed by Snider and Zhou on the basis of the fungal metabolite mutolide **3** (a) and on the basis of benquoine **4** (b). Incorporation of labelled sodium [1-^{13}C]-acetate and $^{18}O_2$ is displayed for **3**.

elongation oxidative tailoring (Scheme 1C).[9] However, **3** has never been co-isolated from any SCH **1** producing strain.

Co-isolation of SCH **1** with the 14-membered 2,4,8-triene lactone benquoine **4** (Scheme 1C) from *Phomopsis* sp. CMU-LMA suggested **4** to be the true precursor of SCH **1** (ESI Fig. S2†) but to-date the biosynthetic pathway has remained elusive.[3]

SCH **1** is structurally related to the bicyclic polyketide brefeldin A **5** (Scheme 1A) that was isolated from various filamentous fungi such as *Eupenicillium brefeldianum*.[10–12] Brefeldin A differs in that it is a 13-membered macrolide (not 10-membered) that is fused to a cyclopentane (not a 4-hydroxycyclohexenone) at the C-5 (not C-3) junction. Incorporation studies with labelled acetate and atmospheric oxygen established the polyketide origin of brefeldin A **5**.[13–15] As in mutolide **3**, both hydroxyl groups of **5** are derived from atmospheric oxygen (Scheme 1A).[14] Tang and co-workers identified the biosynthetic gene cluster (BGC) responsible for the production of **5** in *Eupenicillium brefeldianum*.[12] The *bref* BGC encodes a highly reducing polyketide synthase (hrPKS, *brefPKS*), a thiohydrolase (*brefTH*) and four cytochrome P450 oxygenases (Scheme 1B).[12]

Reconstitution of BrefPKS and the partnering thiohydrolase BrefTH in yeast and *in vitro* led to production of an acyclic 2,4,10-triene octaketide as the dominant product, which possesses the same chain length (C_{16}) and expected β-reduction pattern for formation of **5** (ESI Fig. S3†).[12] It is notable that in the absence of BrefTH, BrefPKS is a nonaketide synthase and the thiohydrolase plays a critical role in chain length control. Subsequent intramolecular annulation and macrolactonization were proposed to give rise to the bicyclic carbon skeleton of **5**.[12] However, the mechanism and timing of both macrolactonization and cyclopentane formation are not yet understood and pose intriguing biosynthetic questions. We reasoned that SCH **1** biosynthesis might proceed in a similar fashion. Here, we report the discovery of the *sch* BGC responsible for formation of SCH **1**. Targeted gene knockout experiments together with heterologous expression of key biosynthetic genes in the fungal host *Aspergillus oryzae* NSAR1 identified a likely minimal gene set needed for production of SCH **1** and shed light on a series of oxidoreductions in the biosynthetic pathway.

Results

Analysis of wild type *Phomopsis* sp. CMU-LMA

In previous work SCH **1** was co-isolated together with a range of polyketide compounds from the large-scale fermentation of *Phomopsis* sp. CMU-LMA wildtype (WT, Fig. 1).[3,16] Here, repeated small-scale cultivation of the WT strain and analysis of ethyl acetate extracts by liquid-chromatography mass spectrometry (LCMS) confirmed reliable production of SCH **1**. SCH **1** was concomitantly produced with LMA P3 **6** and DHTO **7** (Fig. 1). LMA-P1 **8**, a reduced congener of SCH **1**, as well as LMA-P2 **9**, cytosporone B **10** and phomolide C[17] **11** were observed sporadically across fermentation of WT and knockout strains alike and formation of these metabolites appears to be highly sensitive to small changes in culture conditions. The previously reported compounds benquinol **12**, DHTTA **13** and benquoine **4**
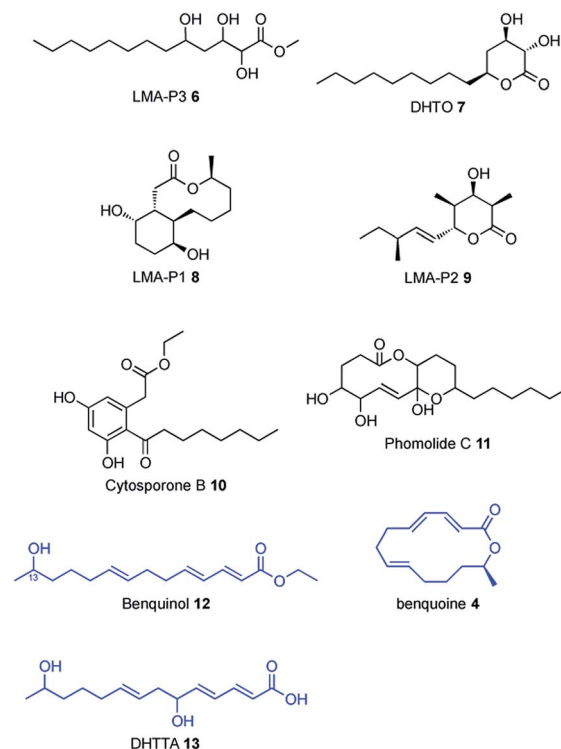

Fig. 1 Secondary metabolites concomitantly isolated with SCH **1**. Compounds in blue were previously isolated from *Phomopsis* sp. CMU-LMA but not observed in this study.

were never observed in this study, possibly as a result of the small-scale cultivation deployed here.

In order to discover the biosynthetic origin of **1** we fed sodium [1-^{13}C]-labelled acetate (Scheme 1A) to the WT strain. Labelled SCH **1** (1 mg) was isolated and analysed by ^{13}C nuclear magnetic resonance (NMR). Isotopic labelling resulted in signal enhancement of seven carbons atoms in SCH **1** (C-1, C-3, C-5, C-7, C-9, C-11, C-13; Scheme 1A and ESI Fig. S4†). As expected, the obtained alternating pattern of isotopic labelling indicated that SCH **1** is formed from seven acetate/malonate units and is consistent with a highly reduced heptaketide without rearrangement. Attachment of the hydroxyl group to the $C_β$-4 carbon indicates that at least one post-elongation oxidative event occurs during **1** biosynthesis, in analogy to incorporation of both hydroxyl groups in **3** and **9** from atmospheric oxygen.[9,14] Notably, the *Z*-configured C-5/C-6 olefin lies within one of the seven acetate units and it thus cannot have been created by the DH domain of the PKS.[18]

Genome analysis of *Phomopsis* sp. CMU-LMA

Genomic DNA of *Phomopsis* sp. CMU-LMA was sequenced (4 × 36 cycles) using the v5 Sequencing Kit (FC-104-5001, Illumina) and assembled by the CASAVA-1.8 data analysis pipeline. A draft genome sequence of 64.4 Mb on 2042 scaffolds with scaffold N50 of 69 395 bp was afforded (for assembly data see ESI Table S1†). Analysis of the genome using the Antibiotics & Secondary Metabolite Analysis Shell (AntiSMASH)[19] identified more than 150 putative secondary metabolite biosynthetic gene

clusters (BGC, ESI Table S2†). Of these, 60 were proposed to encode a PKS as the core gene and manual analysis using the Basic Local Alignment Search Tool (BLAST)[20] predicted 36/60 to belong to the class of highly reducing PKS.[1] Based on the structural resemblance between SCH **1** and brefeldin A **5** we assumed that the PKS responsible for formation of SCH **1** should share sequence homology to *brefPKS*. Indeed, homology searches using *brefPKS* against the *Phomopsis* draft genome sequence identified a putative *sch* BGC centred around a highly reducing PKS (65% global identity to brefPKS). Domain analysis of the putative *schPKS* revealed the expected set of reducing domains and absence of a *C*-methyl transferase (*C*-MeT) domain, consistent with the production of a non-methylated highly reduced polyketide. Manual annotation using Softberry FGENESH[21] and BLAST of open reading frames within the 50 kbp flanking regions of the putative *schPKS* revealed several genes putatively involved in secondary metabolism encoding a hydroxylase (*schR1*); two cytochrome P450 oxygenases (*schR2* and *schR3*); a serine-hydrolase (*schR4*); an NAD dependent

oxidoreductase (*schR5*); a transporter (*schR6*) and an FAD dependent oxidase (*schR7*, Scheme 1B). In the course of this study the genome of *Penicillium verrucosum*, another producer of SCH **1**, became publicly available. Local BLAST analysis against the genome of *P. verrucosum* using *sch* PKS as a template revealed a third homologous cluster centred around an hrPKS (here named *pvschPKS*; 51% global identity to BrefPKS), which contains a similar manifest of genes as observed in the putative *sch* BGC.

A homology analysis was performed between the known *bref* BGC and the two putative *sch* BGC from *Phomopsis* sp. CMU-LMA and *Penicillium verrucosum* using the Artemis comparison tool (ACT),[22] revealing high overall similarity (Scheme 1B). In addition to the hrPKS all clusters share a conserved homologue encoding the thiohydrolase *brefTH* gene (*schR1* and *pvschR1*). A number of homologous cytochrome P450 oxygenases were identified in the three clusters with SchR2 and SchR3 displaying homology to only one P450 (*pvschR3*) in *P. verrucosum* but to three P450s in *P. brefeldianum* (ORF3, ORF4,
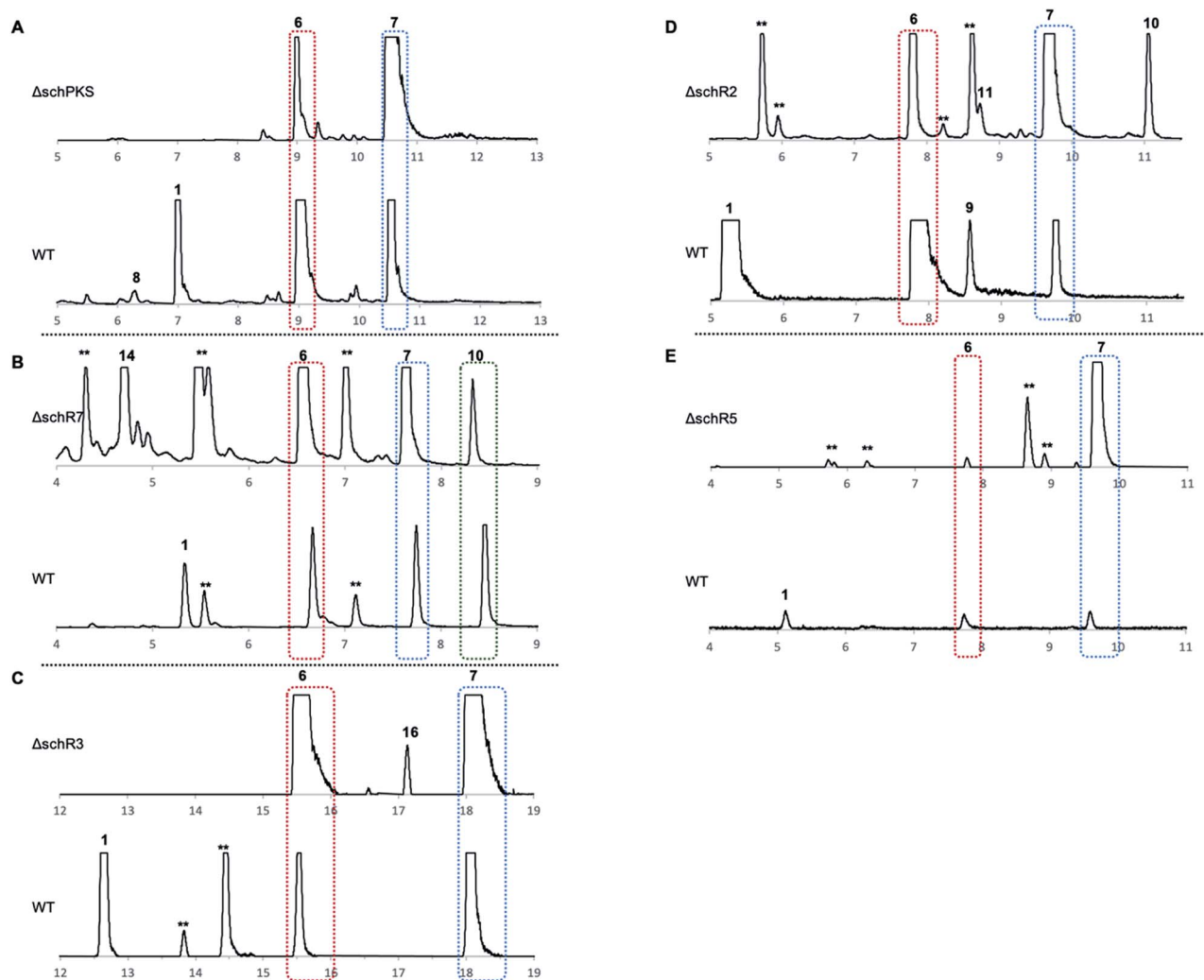

Fig. 2 Targeted gene disruption in *Phomopsis* sp. CMU-LMA. ELSD chromatograms of KO mutants for: (A) *schPKS*; (B) *schR7*; (C) *schR3*; (D) *schR2*; (E) *schR5*. ** = unrelated to SCH **1** biosynthesis. *X*-axis in minutes throughout.

ORF6). The presence of an oxidase encoding gene (*schR7/pvschR2*) is unique to the SCH **1** producing strains and not identified in the *bref* BGC. In order to link the putative *sch* BGC to the biosynthesis of **1** we next attempted targeted knockout experiments.

Targeted gene knockout in *Phomopsis* sp. CMU-LMA

Cultivation of *Phomopsis* sp. CMU-LMA on growth media supplemented with different antibiotics showed that hygromycin B effectively inhibited growth of the WT at 50 μg ml^{-1}. A transformation protocol based on generation of *Phomopsis* protoplasts and insertion of a gene cassette comprising the fungal constitutive *A. nidulans gdpA* promoter (P_{gpdA}) fused to the hygromycin-resistance conferring gene *hph* from *E. coli* was successfully established (ESI Fig. S5†).[23] The bipartite knock-out (KO) method developed by Nielsen and co-workers was then deployed to target genes putatively involved in the biosynthesis of SCH **1**.[24] A total of 137 transformants targeting five biosynthetic genes (*schPKS*, *schR2*, *schR3*, *schR5*, and *schR7*) were obtained and polymerase chain reaction (PCR) successfully confirmed 10 transformants to be true KO strains (ESI Fig. S6†). KO of the serine hydrolase *schR4* was attempted but not successful. All obtained KO strains were cultivated under producing conditions alongside WT *Phomopsis* as a positive control and ethyl acetate extracts of fungal cultures were analysed by LCMS.

Targeted gene KO of *schPKS* (*ΔschPKS*) followed by LCMS analysis showed loss of SCH **1** production and thus linked the *sch* BGC to the biosynthesis of **1** (Fig. 2A). The *ΔschPKS* KO strains were also incapable of producing LMA-P1 **8**, consistent with previous biotransformation experiments that suggested **8** to be a reduced congener of SCH **1** that has undergone both olefin and carbonyl reduction.[25] In contrast, the ongoing capability of Δ*schPKS* KO strains to produce LMA-P3 **6** and DHTO **7** showed these to be biosynthetically unrelated.

KO of the oxidase encoding gene *schR7* (Δ*schR7*), unique to the *sch* BGC and not present in the *bref* BGC, showed loss of SCH **1** production (Fig. 2B). Instead of **1**, formation of a new compound **14** (Scheme 2) was observed. This was purified to homogeneity (2.7 mg). High-resolution mass spectrometry (HRMS) data suggested a molecular formula of $C_{14}H_{20}O_4$ ([M]H$^+$ calculated $C_{14}H_{21}O_4$ 253.3180, found 253.3178). ^{1}H-NMR confirmed **14** to be a macrolactone as the C-14 methyl showed as a clear doublet at 1.26 ppm. Further analysis using ^{1}H–^{1}H-correlation spectroscopy (COSY) confirmed the carbon skeleton of **14** and showed the same atom connectivity and oxidation pattern as observed in the literature for the known 14-membered lactones mutolide **3** and nigrosporolide **15** (ESI Fig. S7–S10 and ESI Table S3†).[9,26] Macrolides **3** and **15** only differ in the configuration of the three olefins, with **3** displaying an *E,E,E* configuration and **15** an *E,Z,Z* geometry. However, small differences in chemical shifts between all three compounds suggested **14** to display an alternative olefin configuration. The coupling constant of the coupled protons H-2 and H-3 (J_{HH} 15.6 Hz) indicated *E*-configuration of this alkene. Coupling constants between the coupled protons H-5 and H-6
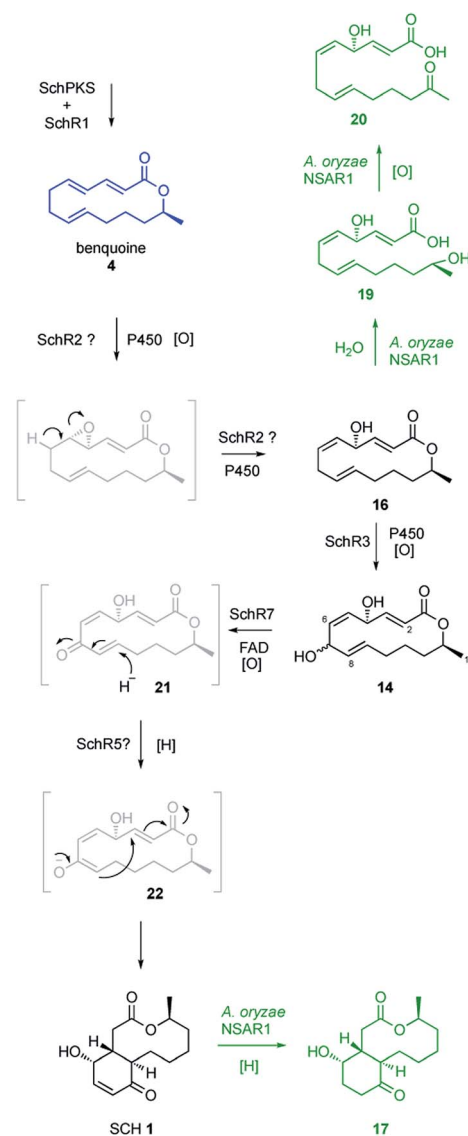
Scheme 2 Proposed biosynthesis of SCH **1** and route to shunt metabolites (green). Compounds in black were isolated in this study, compounds in blue were previously isolated from *Phomopsis* sp. CMU-LMA. Compounds in grey were not observed but suggested as plausible intermediates on the pathway to **1**.

were difficult to determine due to signal overlap with proton H-9. Selective decoupling of H-4, however, led to more accurate peak assignment and allowed determination of a smaller coupling constant for H-5/H-6 (J_{HH} 11.3 Hz), corresponding to a *Z*-configuration (ESI Fig. S11†). The assigned *Z*-configuration is consistent with literature data for the H-5/H-6 *Z*-configuration observed in nigrosporolide **15** (J_{HH} 11.4 Hz). Further decoupling of H-10 simplified determination of the coupling constant between the olefin protons H-8 and H-9 (J_{HH} 15.1 Hz), indicating an *E*-configuration (ESI Fig. S12†). In contrast, the reported *Z*-configuration in nigrosporolide **15** at the alkene protons H-8 and H-9 is reflected by a significantly smaller coupling constant (J_{HH} 10.6 Hz).[25] Further selective decoupling of H-7 did not affect the ^{1}H-signal for H-8, suggesting the dihedral angle

Paper

between the vicinal protons H-7/H-8 to be around 90° and completing the structural elucidation of **14** (ESI Fig. S12†). Accordingly, disruption of *schR7* halted SCH **1** biosynthesis after macrolactonization but prior to annulation.

Next, we investigated the roles of the two cytochromes P450 (*schR2* and *schR3*) in the biosynthesis of **1**, assuming these might be responsible for sequential incorporation of the two hydroxyl groups at the C-4 and C-7 positions. Targeted gene KO of *schR3* (*ΔschR3*) and analysis of ethyl acetate extracts of transformants by LCMS showed that production of SCH **1** was abolished (Fig. 2C). Instead, a less polar compound **16** emerged (Scheme 2), consistent with interrupting the biosynthetic pathway towards **1** at a less oxidized state. HRMS analysis confirmed a molecular formula of $C_{14}H_{20}O_3$ ([M]H$^+$ calculated $C_{14}H_{21}O_3$ 237.3185, found 237.3181). Purification to homogeneity afforded 0.8 mg of **16**, the structure of which was elucidated by full NMR analysis (ESI Fig. S13–S17 and ESI Table S4†). The obtained NMR data indicated structural similarity to **14** and a 16 amu difference in HRMS data suggested **16** to be the dehydroxyl analogue of **14**. Indeed, replacement of the downfield shifted oxygenated proton in **14** (δ_H/δ_C 4.82/70.6 ppm, for H-7/C-7) by two upfield shifted aliphatic protons in **16** (δ_H/δ_C 2.82/32.1 ppm, for H_2-7/C-7) was clearly observed in the NMR data and together with further COSY and HMBC data confirmed the structure of **16**. Observation of **16** conclusively suggests *schR3* to incorporate the C-7 hydroxyl group observed in SCH **1** and to act prior to *schR7*.

Inactivation of the second cytochrome P450 *schR2* (*ΔschR2*) yielded transformants that were deficient in the production of SCH **1** and LMA-P1 **7** (Fig. 2D). However, no new intermediates and neither compounds **14** nor **16** were observed in these strains, indicating that SchR2 acts prior to SchR3 and SchR7 and that the pathway is halted in absence of *schR2* at an early biosynthetic stage. Formation of phomolide C **11** and cytosporone B **10** was observed in the *ΔschR2* mutant but not assumed to be SCH **1** intermediates due to their structure and unpredictable appearance in WT strains when grown under identical conditions.

Finally, targeted gene disruption of *schR5*, an oxidoreductase unique to the *sch* BGC, yielded two true KO transformants. LCMS analysis of these strains under producing conditions showed that production of **1** and **8** was abolished but no new compounds were observed (Fig. 2E). Together, the targeted gene KO experiments identified five genes (*schPKS*, *schR2*, *schR3*, *schR5*, *schR7*) that are essential for the biosynthesis of SCH **1**.

Reconstitution of SCH biosynthesis in *Aspergillus oryzae* NSAR1

To further investigate the function of individual genes we attempted reconstitution of the SCH biosynthetic pathway in the fungal host *A. oryzae* NSAR1.[27] As SCH **1** was previously shown to be transformed by *Aspergillus ochraceus* ATCC 1009 resting cells into several reduced congeners[24] we first conducted a biotransformation experiment to assess the stability of SCH **1** in *A. oryzae*. SCH **1** was fed to a growing culture (2 d) of *A. oryzae* NSAR1. Extraction at day 5 and analysis of extracts by LCMS

showed that **1** was predominantly transformed into compound **17** (Fig. 3A). A minor co-metabolite, compound **18**, with identical mass fragmentation pattern and UV absorption as **17** was also observed but eluded characterization due to low production titres (ESI Fig. S18†).

Isolation of the component **17** and purification to homogeneity afforded 1.2 mg (HRMS $C_{14}H_{22}O_4$ [M − H]$^-$ calculated $C_{14}H_{21}O_4$ 253.1440, found 253.1440). A 2 amu difference in HRMS compared to SCH **1** suggested **17** to be a reduced congener of **1**. Indeed, full NMR analysis identified **17** as the same SCH congener that was previously obtained upon biotransformation of SCH **1** with *Aspergillus ochraceus* (ESI Fig. S19–S23 and ESI Table S5†).[24] Contrary to SCH **1**, the C_5–C_6 olefin in **17** is reduced.

A series of fungal expression plasmids were constructed to express different combinations of *sch* biosynthetic genes in *A. oryzae*. For this, cDNA was prepared from *Phomopsis* WT under producing conditions and yeast homologous recombination was used to clone biosynthetic genes into the modular expression system described by Lazarus and co-workers.[28]

Plasmids corresponding to the "full" SCH biosynthetic gene cluster (*schPKS*, *schR1*, *schR2*, *schR3*, *schR4*, *schR5*, *schR7*, but omitting the transporter *schR6*) were successfully transformed into *A. oryzae*. Biotransformation of **1** by *A. oryzae* WT indicated that successful reconstitution of the *sch* BGC in the heterologous host should yield the reduced SCH analogue **17** instead of **1**. Indeed, growth under inducing conditions and LCMS analysis of transformants carrying the full cluster showed production of trace amounts of **17** and the minor co-metabolite **18**
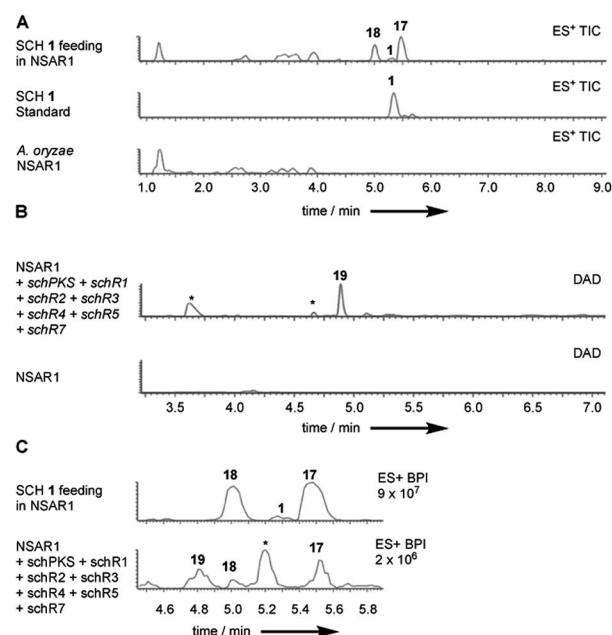

Fig. 3 (A) Biotransformation of SCH **1** by *A. oryzae* NSAR1. ES$^+$ traces of fed **1** to *A. oryzae*, a standard of **1** and WT control; (B) heterologous expression of the full *sch* BGC. Diode array detector (DAD) traces of pathway expression and WT control; (C) heterologous expression of the full *sch* BGC and comparison to fed **1** to *A. oryzae*. ES$^+$ traces of fed **1** (top) and full *sch* BGC (bottom).

previously observed in biotransformation experiments (Fig. 3C). SCH **1** was not observed.

Observation of trace amounts of **17** upon expressing the "full" *sch* BGC shows that the transformed set of genes is sufficient for production of **1** and that no other gene is needed for SCH **1** biosynthesis. However, transformation of the full cluster also yielded **19** as the dominant product and **20** as a minor co-metabolite (Fig. 3B and ESI Fig. S24†). Isolation of **19** and purification to homogeneity (1 mg; HRMS [M − H]⁻ calculated $C_{14}H_{21}O_4$ 253.1440, found 253.1440) followed by NMR characterization revealed a high similarity to data previously obtained for compound **16** (ESI Fig. S25–S29 and ESI Table S6†), obtained upon KO of *schR3*. An 18 amu difference observed in HRMS indicated addition of water in the case of **19**, consistent with an opened lactone. Indeed, significant differences in chemical shifts of the methyl group protons at C-14 (δ_{H3-14} 1.02 ppm in 19, δ_{H3-14} 1.27 ppm in **16**) and upfield shift of the proton attached to C-13 (δ_{H-13} 3.56 ppm in 19, δ_{H-13} 4.82 ppm in **16**) supported **19** to be the open acid form of **16**. Bromocresol staining of **16** and **19** supported **19** to be the corresponding free acid derivative of **16** (ESI Fig. S30†). The coupling constant (J_{HH} 15.4 Hz) of the alkene protons H-2/H-3 indicated 2*E*-configuration. Determination of the coupling constant between olefin protons H-5 and H-6 was difficult due to overlapping ¹H-signals with H-8 and H-9. ¹H-decoupling of H-7 facilitated determination of the coupling constant of the olefin protons H-5/H-6 (J_{HH} 10.8 Hz) and suggested a *Z*-configuration (ESI Fig. S31†). Further decoupling of H-10 allowed determination of the coupling constant for the alkene protons H-8/H-9 (J_{HH} 15.4 Hz) and suggesting an *E*-olefin (ESI Fig. S32†). The observed double bond configurations were consistent with the configurations determined for compound **16**.

Purification of compound **20** to homogeneity (1.9 mg) and subsequent NMR analysis revealed almost identical chemical shifts compared to **19** (ESI Fig. S33–S37 and ESI Table S7†). However, C-13 was identified as a quaternary position as observed by heteronuclear single quantum coherence spectroscopy (HSQC) and the corresponding chemical shift of C-13 (208.3 ppm) indicated a carbonyl group instead of an alcohol, agreeing with HRMS data obtained for **20** ([M − H]⁻ calculated $C_{14}H_{19}O_4$ 251.1283, found 251.1286). Compound **20** thus constitutes the 13-keto-congener of **19**. Since gene disruption of *schR3* and *schR7* yielded the intact lactones **14** and **16**, observation of **19** and **20** suggests these to be early shunt products, probably derived by early hydrolysis of the lactone moiety in **16**.

Expression of early genes in *A. oryzae*

To investigate early steps in SCH **1** biosynthesis we attempted to assemble the pathway stepwise, starting with expression of the standalone *schPKS*. But neither expression of *schPKS* alone nor co-expression with thiohydrolase encoding gene *schR1* revealed any early biosynthetic intermediates (ESI Fig. S38†) in *A. oryzae*. Full cluster expression and observation of compound **17** however had previously demonstrated that SchPKS is active in *A. oryzae*. We thus assumed that the PKS product is likely to be shunted in this fungal host. This is consistent with the previous
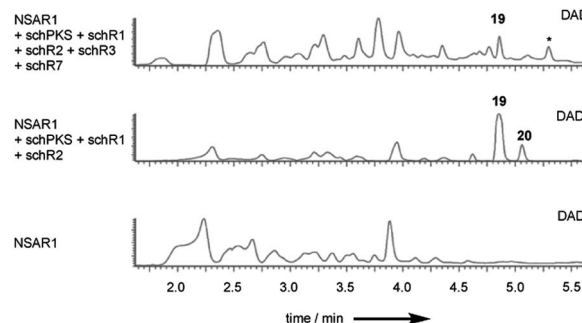

Fig. 4 DAD chromatograms of fungal extracts from the heterologous expression of early biosynthetic genes in *A. oryzae* NSAR1. Top, co-expression of *schPKS*, *schR1*, *schR2*, *schR3*, *schR7*; middle, co-expression of *schPKS*, *schR1*, *schR2*; bottom, NSAR1 WT.

finding that upon KO of *schR2* no intermediates are observed, suggesting that the early intermediates of SCH **1** biosynthesis are quickly degraded. This is consistent with previous observations of rapid degradation of linear (non-methylated) polyketides in *Aspergillus oryzae*, probably by β− or ω-oxidation.[29]

Inclusion of the P450 *schR2* in the expression affords acyclic compounds **19** and **20** again, but no trace amounts of **17** were identified (Fig. 4). This is consistent with SchR2 introducing the C-4 hydroxyl group prior to the pathway being redirected into the shunt pathway. Addition of oxidase encoding gene *schR7* and the second P450 encoded by *schR3* gave **19** and **20** but at lower titre. Together these results show that SchPKS, the partnering hydrolase SchR1 and one of the two P450s are sufficient to produce the **16** analogue **19** which is probably a shunt product in *A. oryzae*. Further oxidation by the heterologous host results in **20**.

Finally, omission of *schR1*, the thiohydrolase encoding gene, from the full cluster expression abolishes production of any SCH **1** congener (ESI Fig. S39†) as expected from the brefeldin A pathway.[12]

Discussion and conclusion

In this study the Sch-642305 BGC (*sch* BGC) was discovered and validated. Reconstitution of the entire SCH **1** biosynthetic gene cluster in *A. oryzae* NSAR1 successfully afforded the biotransformed SCH **1** congener **17** and demonstrated that a minimal set of 7 genes is sufficient to produce **1**. Early steps in SCH **1** biosynthesis eluded characterization as gene disruptions in the native producer did not lead to formation of early stage biosynthetic intermediates. Likewise, investigation of early steps in *A. oryzae* repeatedly led to formation of the acyclic SCH **1** congeners **19** and **20**. We assume that **19** and **20** constitute shunt products derived by hydrolysis of the lactone **16** by the heterologous host. Unexpected and undesired side reactions upon heterologous expression in *A. oryzae* are well-known. Oikawa and coworkers *e.g.* previously reported undesired oxidative shunting upon expressing key biosynthetic genes involved in cytocholasin K and solanapyrone formation.[30,31] Similar oxidations have been described for the heterologous

expression of desmethylbassianin and for the avirulence gene ACE1.[32,33] All observed oxidations occurred at the terminus of linear polyketide precursors such as the observed oxidation of compound **19** to **20**.

Given the high homology between the *sch* BGC and the *bref* BGC we believe it is reasonable to assume that early biosynthetic steps are similar. Tang and co-workers showed that reconstitution of the hrPKS BrefPKS and the thiohydrolase BrefTH led to formation of an acyclic octaketide likely to be the precursor of **5**, with formation of the correct octaketide being dependent on the presence of the thiohydrolase BrefTH.[12] They proposed a mechanism where the thiohydrolase BrefTH performs both off-loading of the PKS chain and lactonization by using its catalytic His-276 to deprotonate the terminal hydroxyl group of the linear octaketide and thus yielding a suitable nucleophile for lactonization. It is easy to imagine how small changes in PKS programming lead to formation of a heptaketide in **1** biosynthesis in contrast to the octaketide observed in **5** biosynthesis and we propose that a similar interplay between SchPKS and SchR1 gives rise to such early intermediates. Co-isolation of benquinol **12** and benquoine **4** from the SCH **1** producing strain *Phomopsis* sp. CMU-LMA indeed identified such likely early biosynthetic intermediates. Deprotonation of the C-13 hydroxyl group of **12** would indeed give rise to a suitable nucleophile for **4** formation. A similar mechanism was recently proposed for the fungal macrolides phaeospelide A and phaseolide A where macrolactone formation was solely dependent on the associative work of a hrPKS and a standalone *trans* acting thiolesterase.[34]

Furthermore, omission of s*chR1* from the heterologous expression in *A. oryzae* abolished production of any SCH congeners and thus demonstrates the crucial role it plays in SCH biosynthesis. The obtained data from KO experiments suggest that the two cytochrome P450 oxygenases SchR2 and SchR3 subsequently introduce the C-4 and C-7 hydroxyl groups. SchR2 most likely acts on the C-4/C-5 *E*-configured olefin inserting an epoxide which can open to the isolated compound **16** with consequent double bond migration. Subsequent action of SchR3 inserts the C-7 hydroxyl and gives rise to the observed intermediate 14 (Scheme 2).

The key structural feature of SCH **1** is the presence of the 4-hydroxycyclohexenone ring, formation of which is not yet understood. Based on the results obtained from KO experiments and heterologous expression experiments functions have been assigned to all genes except *schR5* and *schR7*, suggesting one of these to be responsible for formation of the six-membered ring. Bioinformatic analysis of schR7 shows highest homology (28% sequence identity) to the flavoprotein 6-hydroxy-D-nicotine oxidase from *Neurospora crassa*, an enzyme known to convert hydroxyl groups to ketones and we thus propose SchR7 to catalyse conversion of the C-7 hydroxyl group in **14** to the corresponding ketone **21** (Scheme 2). Putative reduction of the C-5/C-6 olefin by oxidoreductase SchR5 would lead to formation of the enolate **22** which could undergo subsequent Michael-type cyclization to generate the 4-hydroxycyclohexenone ring observed in SCH **1**. Disruption of the *schR5*

gene abolished production of **1** and thus it has to play a crucial role in **1** formation.

It is notable that the timing of formation of the 4-cyclohexenone moiety in SCH **1** must differ from formation of the cyclopentane ring observed in brefeldin A **5**. Observations by Tang and co-workers that reconstitution of BrefPKS and BrefTH affords acyclic PKS products only suggests that cyclopentane formation needs to occur prior to macrolactonization, thus generating a configuration more favourable for lactone formation.[12] On the contrary, in SCH **1** biosynthesis lactone formation occurs prior to formation of the six-membered ring, as indicated by observation of the lactones **14** and **16** which lack the cyclohexenone moiety. Additionally, during SCH **1** biosynthesis we conclusively demonstrated that both C-4 and the C-7 hydroxylation occur prior to formation of the cyclohexenone moiety whereas labelling studies by Hutchinson and co-workers suggest that ring closure in **3** is not dependent on C-7 hydroxylation.[13]

Overall, we have identified the *sch* BGC in *Phomopsis* sp. CMU-LMA, and shown key steps of the biosynthesis are similar to those proposed for brefeldin A **5**, although the trans-annulation steps differ. This is consistent with differences in the respective gene clusters. Combined data from gene disruptions and reconstitution of SCH **1** biosynthesis in *A. oryzae* suggest a minimal gene set needed for formation of **1** and a plausible pathway towards **1** was suggested for the first time. Further work will be required to conclusively demonstrate the mechanism of ring formation.

Conflicts of interest

There are no conflicts to declare.

Acknowledgements

Notes and references

1 R. J. Cox, *Org. Biomol. Chem.*, 2007, **5**, 2010–2026.
2 M. Chu, R. Mierzwa, L. Xu, L. He, J. Terracciano, M. Patel, V. Gullo, T. Black, W. Zhao, T.-M. Chan and A. T. McPhail, *J. Nat. Prod.*, 2003, **66**, 1527–1530.
3 E. Adelin, C. Servy, S. Cortial, H. Lévaique, M.-T. Martin, P. Retailleau, G. Goff, B. Bussaban, S. Lumyong and J. Ouazzani, *Phytochemistry*, 2011, **72**, 2406–2412.
4 H. Jayasuriya, D. L. Zink, J. D. Polishook, G. F. Bills, A. W. Dombrowski, O. Genilloud, F. F. Pelaez, L. Herranz,

D. Quamina, R. B. Lingham, R. Danzeizen, P. L. Graham, J. E. Tomassini and S. B. Singh, *Chem. Biodiversity*, 2005, **2**, 112–122.

5 G. Mehta and H. M. Shinde, *Tetrahedron Lett.*, 2005, **46**, 6633–6636.

6 G. Mehta and H. M. Shinde, *Chem. Commun.*, 2005, 3703.

7 E. M. Wilson and D. Trauner, Concise Synthesis of the Bacterial DNA Primase Inhibitor (+)-Sch 642305, *Org. Lett.*, 2007, **9**, 1327–1329.

8 B. B. Snider and J. Zhou, *Org. Lett.*, 2006, **8**, 1283–1286.

9 H. B. Bode, M. Walker and A. Zeeck, *Eur. J. Org. Chem.*, 2000, **2000**, 1451–1456.

10 V. L. Singleton, N. Bohonos and A. J. Ullstrup, *Nature*, 1958, **181**, 1072–1073.

11 Y. Suzuki, H. Tanaka, H. Aoki and T. Tamura, *Agric. Biol. Chem.*, 1970, **34**, 395–413.

12 A. O. Zabala, Y.-H. Chooi, M. Choi, H.-C. Lin and Y. Tang, *ACS Chem. Biol.*, 2014, **9**, 1576–1586.

13 Y. Yamamoto, A. Hori and C. R. Hutchinson, *J. Am. Chem. Soc.*, 1985, **107**, 2471–2474.

14 C. T. Mabuni, L. Garlaschelli, R. A. Ellison and C. R. Hutchinson, *J. Am. Chem. Soc.*, 1979, **101**, 707–714.

15 B. E. Cross and P. Hendley, *J. Chem. Soc., Chem. Commun.*, 1975, 124b–1125.

16 E. Adelin, M.-T. Martin, S. Cortial, P. Retailleau, S. Lumyong and J. Ouazzani, *Phytochemistry*, 2013, **93**, 170–175.

17 A. Ito, H. Maeda, A. Tonouchi and M. Hashimoto, *Biosci., Biotechnol., Biochem.*, 2015, **79**, 1067–1069.

18 D. H. Kwan and F. Schulz, *Molecules*, 2011, **16**, 6092–6115.

19 K. Blin, S. Shaw, K. Steinke, R. Villebro, N. Ziemert, S. Lee, M. H. Medema and T. Weber, *Nucleic Acids Res.*, 2019, **47**, W81–W87.

20 S. F. Altschul, W. Gish, W. Miller, E. W. Myers and D. J. Lipman, *J. Mol. Biol.*, 1990, **215**, 403–410.

21 A. A. Salamov and V. V. Solovyev, *Genome Res.*, 2000, **10**, 516–522.

22 T. J. Carver, K. M. Rutherford, M. Berriman, M.-A. Rajandream, B. G. Barrell and J. Parkhill, *Bioinformatics*, 2005, **21**, 3422–3423.

23 P. J. Punt, R. P. Oliver, M. A. Dingemanse, P. H. Pouwels and C. A. M. J. J. van den Hondel, *Gene*, 1987, **56**, 117–124.

24 M. L. Nielsen, L. Albertsen, G. Lettier, J. B. Nielsen and U. H. Mortensen, *Fungal Genet. Biol.*, 2006, **43**, 54–64.

25 E. Adelin, C. Servy, S. Cortial, H. Lévaique, J. Gallard, M.-T. Martin, P. Retailleau, B. Bussaban, S. Lumyong and J. Ouazzani, *Bioorg. Med. Chem. Lett.*, 2011, **21**, 2456–2459.

26 J. S. Harwooda, H. G. Cutler and J. M. Jacyno, Nigrosporolide, *Nat. Prod. Lett.*, 2006, **6**, 181–185.

27 F. J. Jin, J. Maruyama, P. R. Juvvadi, M. Arioka and K. Kitamoto, *FEMS Microbiol. Lett.*, 2004, **239**, 79–85.

28 M. N. Heneghan, A. A. Yakasai, L. M. Halo, Z. Song, A. M. Bailey, T. J. Simpson, R. J. Cox and C. M. Lazarus, *ChemBioChem*, 2010, **11**, 1508–1512.

29 E. J. Skellam, D. Hurley, J. Davison, C. M. Lazarus, T. J. Simpson and R. J. Cox, *Mol. BioSyst.*, 2010, **6**, 680–682.

30 R. Fujii, A. Minami, K. Gomi and H. Oikawa, *Tetrahedron Lett.*, 2013, **54**, 2999–3002.

31 R. Fujii, T. Ugai, H. Ichinose, M. Hatakeyama, T. Kosaki, K. Gomi, I. Fujii, A. Minami and H. Oikawa, *Biosci., Biotechnol., Biochem.*, 2015, **80**, 426–431.

32 Z. Song, W. Bakeer, J. W. Marshall, A. A. Yakasai, R. Khalid, J. Collemare, E. Skellam, D. Tharreau, M.-H. Lebrun, C. M. Lazarus, A. M. Bailey, T. J. Simpson and R. J. Cox, *Chem. Sci.*, 2015, **6**, 4837–4845.

33 M. N. Heneghan, A. A. Yakasai, K. Williams, K. A. Kadir, Z. Wasil, W. Bakeer, K. M. Fisch, A. M. Bailey, T. J. Simpson, R. J. Cox and C. M. Lazarus, *Chem. Sci.*, 2011, **2**, 972–979.

34 Y. Morishita, H. Zhang, T. Taniguchi, K. Mori and T. Asai, *Org. Lett.*, 2019, **21**, 4788–4792; Y. Morishita, T. Sonohara, T. Taniguchi, K. Adachi, M. Fujita and T. Asai, *Org. Biomol. Chem.*, 2020, **18**, 2813–2816.